

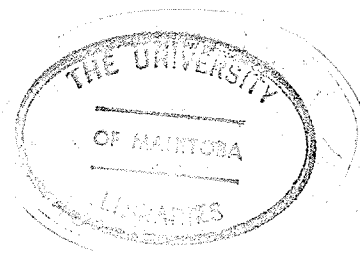
A PROGRAMMABLE DYNAMOMETER

A THESIS
PRESENTED TO
THE FACULTY OF GRADUATE STUDIES AND RESEARCH
UNIVERSITY OF MANITOBA

IN PARTIAL FULFILMENT
OF THE REQUIREMENTS FOR THE DEGREE
MASTER OF SCIENCE
IN ELECTRICAL ENGINEERING

BY
EDWARD ANTHONY ZALESKI

JULY 1966 ✓



ACKNOWLEDGEMENT

The author wishes to express his appreciation to his advisor, Professor G. W. Swift, for his guidance and assistance throughout this work, and to the University of Manitoba for its financial assistance.

TABLE OF CONTENTS

CHAPTER		PAGE
I.	INTRODUCTION	1
II.	THE PROPOSED SYSTEM	4
III.	ANALYSIS OF THE SYSTEM	15
IV.	COMPENSATION OF THE SYSTEM	21
V.	DISCUSSION OF RESULTS AND CONCLUSIONS	30
	BIBLIOGRAPHY	32
	APPENDIX A	33
	APPENDIX B	35

LIST OF FIGURES

FIGURE		PAGE
2-1	The desired output of the system and a possible output achieved.	5
2-2	Block diagram of the proposed system.	6
2-3	Static characteristic of the torque sensor.	7
2-4	Static characteristic of the dynamometer.	9
2-5	Static characteristic of the tachometer.	10
2-6	Schematic diagram of the power amplifier.	11
2-7	Static characteristic of the power amplifier.	12
2-8	Response of a typical component to a step.	13
3-1	Equivalent block diagram of the proposed system.	15
3-2	Phase plane portrait for the system of equation 3-4.	18
3-3	Response of the system to a step input (motor torque equal to zero)	20
4-1	Schematic diagram of the analog computer simulation of the system.	22
4-2	Response of the system to a step input (motor torque equal to zero)	23
4-3	Response of the system to a step with the effects of motor torque included.	24

FIGURE		PAGE
4-4	Response of the system after compensation.	24
4-5	The Integral Squared Error as a function of feedback gain.	25
4-6	Normalized variation of the gain of the system due to the presence of acceleration.	26
4-7	The desired compensating amplifier characteristic.	27
4-8	Response of the compensated system.	27
4-9	Schematic diagram of the compensator.	28
B-1	An illustration of the graphical method for obtaining phase plane trajectories.	36

LIST OF TABLES

Table		Page
2-1	Static characteristic of the torque sensor.	7
2-2	Static characteristic of the dynamometer.	8
2-3	Static characteristic of the tachometer.	10
2-4	Static characteristic of the power amplifier.	11
2-5	Transfer functions of the components.	14
3-1	Calculation of the output torque.	19
4-1	The Integral Squared Error of the compensated system.	28
B-1	Calculation of $-f(x)/C_1$.	37

ABSTRACT

The object of this investigation was to design a system to automatically control the dynamic loading of motors. The Integral Squared Error was used as a criterion for accuracy, and a suitable system was designed using phase plane analysis and analog computer simulation of the system. The final design was found to be suitable for only large values of output.

CHAPTER I

INTRODUCTION

The Problem.

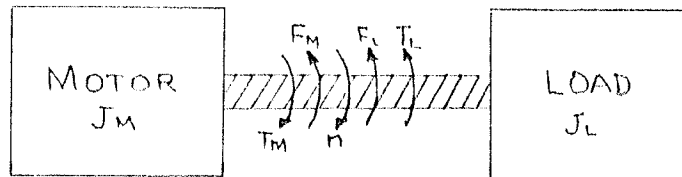
When a motor is being tested under transient conditions (for example during starting), its behavior is dependent on the torque-speed characteristic of the connected load. For example, the torque of a fan load is zero at zero speed and increases non-linearly with increasing speed, whereas the torque of many other loads is roughly constant with respect to speed.

A load such as one of those described above may be statically simulated using a dynamometer and adjusting its torque to a given value at a given speed and proceeding step-by-step over the entire speed range. The object of this investigation was to design a loading device which would dynamically simulate any given load; that is, it would have a prescribed torque-speed characteristic under transient conditions.

Range of Control.

A brief examination of the differential equations of a motor-load system will show the range of control attainable by controlling the load torque.

Consider a motor mechanically coupled to a load.



The motor develops a torque T_m , has an inertia J_m , and a friction torque loss of F_m . Similarly, the load consists of a torque T_L , an inertia J_L , and a friction torque of F_L . The equation governing the motion of the system is

$$T_m = F_m + F_L + T_L + (J_m + J_L) \frac{dn}{dt} \quad 1.1$$

where n is the speed of rotation of the system.

The output torque of the motor (or equivalently the torque supplied to the load) is

$$M = T_m - F_m - J_m \frac{dn}{dt} \quad 1.2$$

Solving equation 1.1 for $\frac{dn}{dt}$ and substituting into equation 1.2 yields

$$M = \left[F_L + (T_m - F_m - F_L) J_L / J_t \right] + \left[F_L (1 - J_L / J_t) \right] \quad 1.3$$

where $J_t = J_m + J_L$

Examination of equation 1.3 reveals that the output torque is made up of two components:

- 1) a fixed term, depending only on the inertias of the system, and the friction and motor torques, and
- 2) a variable term, depending on the value of the load torque.

If the loading device* cannot motor the system, then there is a lower limit to the output torque, given by equation 1.3 with T_L set to zero.

$$T_{\min.} = F_L + (T_m - F_m - F_L) J_L / J_t \quad 1.4$$

Considering only positive acceleration, the maximum output occurs when T_L is such as to make $\frac{dn}{dt}$ equal to zero. From equation 1.2,

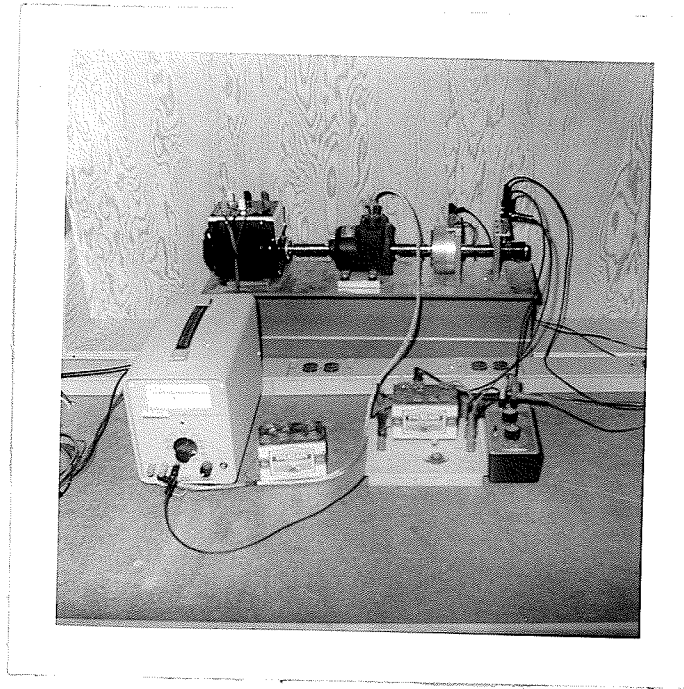
$$T_{\max.} = T_m - F_m \quad 1.5$$

The range of control is therefore given by

$$T_{\min.} \leq M \leq T_{\max.} \quad 1.6$$

In Chapter II, a system will be proposed to accomplish the desired control. The characteristics of the proposed system will also be determined.

* The loading device used in this investigation was a hysteresis brake, hence T_L could never be made negative.



Back row (left to right):

Induction motor, torque sensor, dynamometer, tachometer.

Front row (left to right):

Cohu amplifier, power amplifier.

PHOTOGRAPH OF THE SYSTEM.

CHAPTER II

THE PROPOSED SYSTEM

Specifications of the System

Equation 1.3 shows the relationship between the output torque and the load torque. It should be noted, however, that the independent variable is not given in the equation. In this investigation, it was desired to control the output torque as a function of the speed, n .

Since the output is to be made equal to the input, the input signal will also be a function of speed.

Also, because dynamic loading is considered, acceleration is present, and the accelerating torque will be considered as a disturbance.

As a performance index for the system, the Integral Squared Error will be used. The choice of this as a criterion is arbitrary, but since large errors are weighted, the peak error will also tend to be minimized when minimizing the Integral Squared Error. In equation form, the performance index is then

$$I = \int y(n)^2 dn \leq M \quad 2-1$$

where $y(n)$ is the error as a function of speed and M is the level of accuracy desired.

Figure 2-1 shows a sketch of a desired output of the system and the actual output achieved. The error is shown cross hatched.

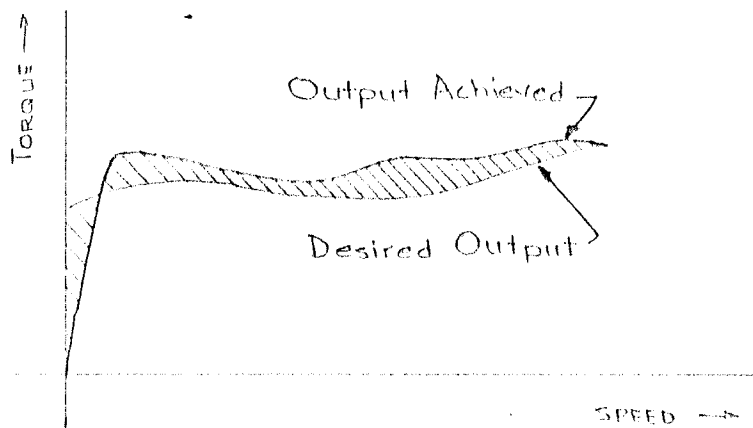


Figure 2-1: The desired output of the system and the possible output achieved.

The proposed system is to be composed basically of a dynamometer*, a torque sensor, a tachometer, a function generator, and electronic amplifiers. The block diagram is shown in Figure 2-2.

In Figure 2-2, the output torque is measured and compared with the input (desired output). The error is then added to the input to give the actuating signal.

* See footnote on page 3.

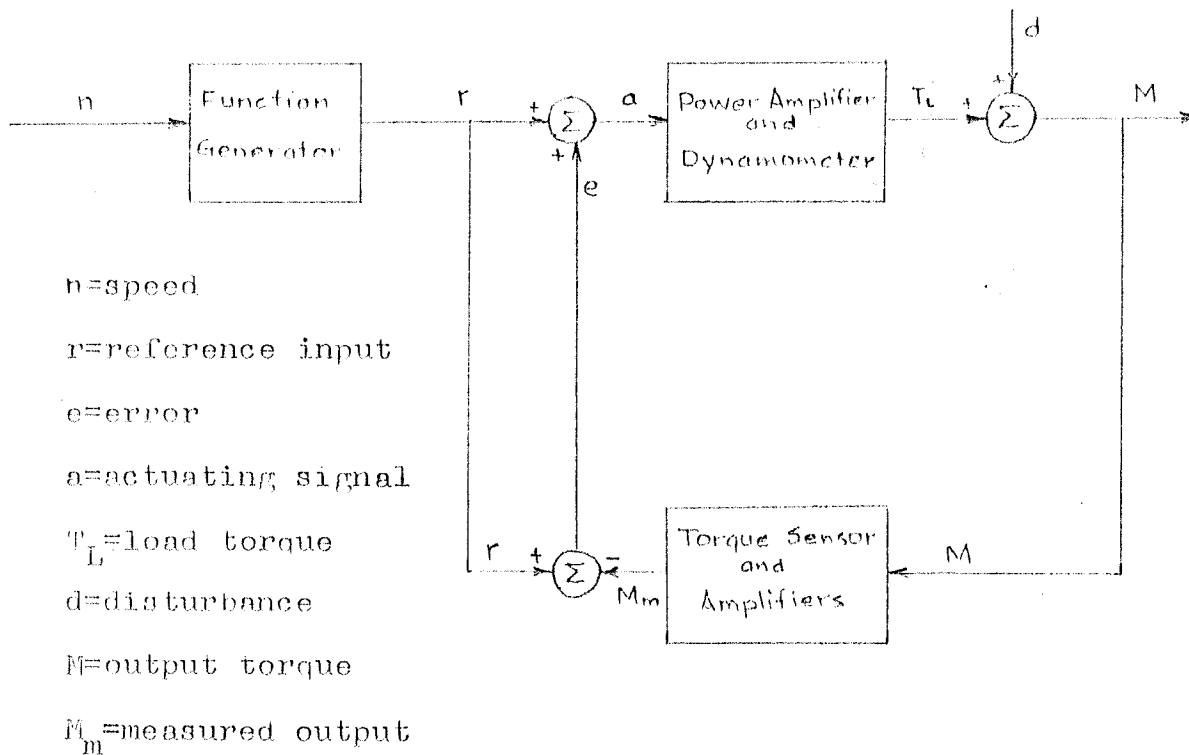


Figure 2-2; Block diagram of the proposed system.

Characteristics of the Components

The nameplate data of the components are given in Appendix A.

A) Static Characteristics

1) Torque Sensor

The torque sensor circuit consists of four strain gauges mounted on a shaft, connected to form a Wheatstone Bridge. The output voltage is a linear function of the product of bridge excitation and applied torque.

Measurements for the characteristic are shown in Table 2-1.

The data of Table 2-1 are plotted in Figure 2-3.

Table 2-1: Static characteristic of the torque sensor.

Applied Torque (in.-oz.)	Output Voltage (m.v.)
0	0.0
10	2.5
20	4.5
30	7.0
40	9.5
50	11.9
60	14.3
70	16.7

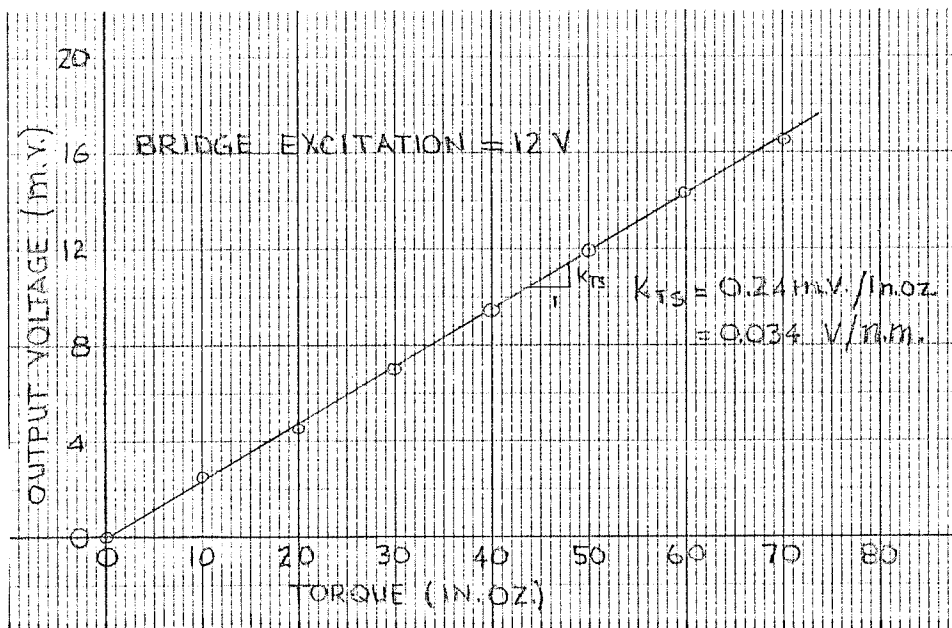


Figure 2-3: Static characteristic of the torque sensor.

2) Dynamometer

The dynamometer is a current sensitive device with the following static characteristic.

Input Current (m.a.)	Output Voltage (m.v.)	Output Torque (in.oz.)	Corrected Output Torque (in.oz.)
0.0	0.48	2.0	0.0
10.0	1.08	4.5	2.5
12.2	1.38	5.8	3.8
15.0	2.11	8.8	6.8
17.5	2.90	12.1	10.1
20.0	3.96	16.5	14.5

The above readings were taken at a constant speed of 1135 r. p. m., and it was found that the readings did not change appreciably with changes in speed.

In obtaining the above readings, the torque sensor characteristic was used. A current was applied to the dynamometer, and the output voltage of the torque sensor measured. The voltage values were then converted to torque readings using the previously obtained characteristic.

The non-zero output with zero input is accounted for by the load friction, F_L . Assuming friction to be independent of speed, the dynamometer characteristic may

be approximated by

$$T_o = K_o I_{in}^2$$

$$\text{where } K_o = 247 \text{ n.m./amp}^2$$

K_o was obtained from Figure 2-4, which shows the corrected output torque readings of Table 2-2 plotted against I_{in}^2 .

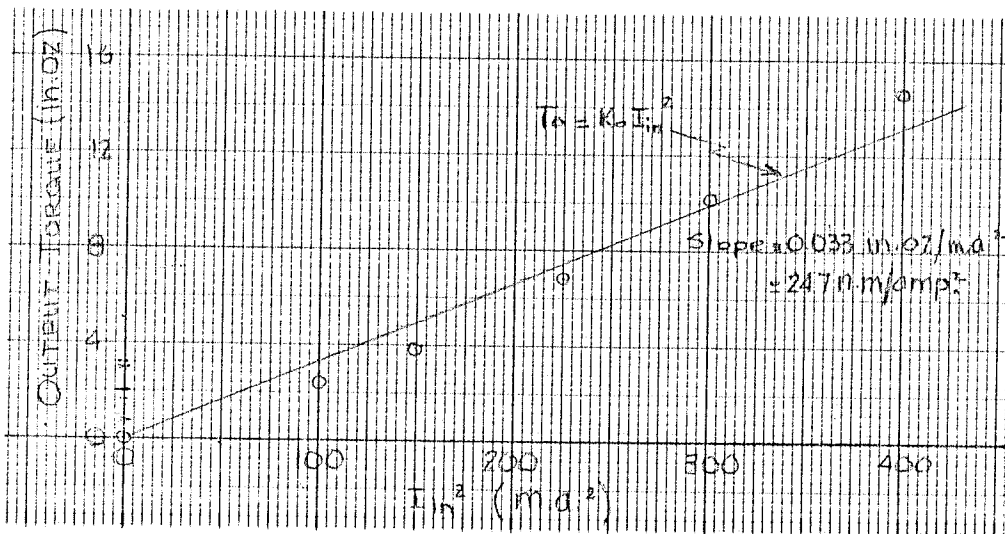


Figure 2-4: Static characteristic of the dynamometer.

3) Tachometer

Readings for the tachometer acharacteristic are shown in Table 2-3, and the data of Table 2-3 are plotted in Figure 2-5.

Table 2-3: Static characteristic of the tachometer.

Speed (r.p.m.)	Output Voltage (volts)
0	0.0
405	2.8
1000	6.8
1465	10.5
1790	12.3

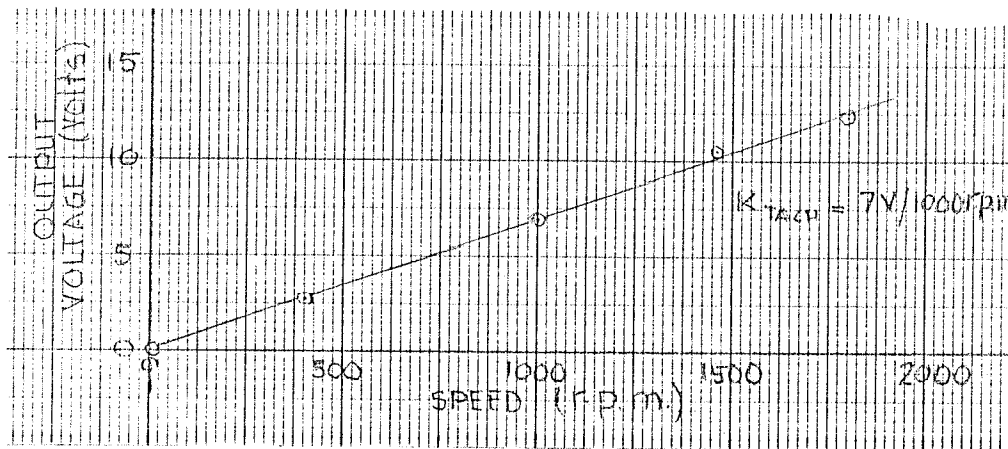


Figure 2-5: Static characteristic of the tachometer.

4) Power Amplifier

Because the dynamometer is a current sensitive device, it is necessary to use a power amplifier in its input stage. The schematic diagram of the amplifier and its static characteristic are shown below.

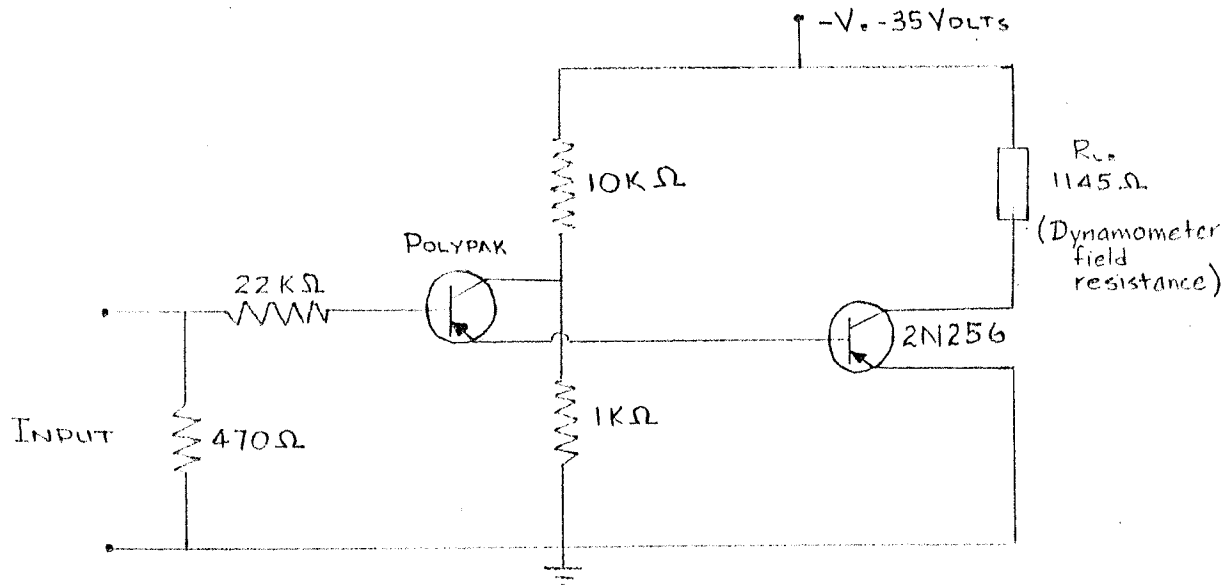


Figure 2-6: Schematic diagram of the power amplifier.

Table 2-4: Static characteristic of the power amplifier.

Input Voltage (volts)	Output Current (m.a.)
0.00	3.5
0.13	5.0
0.21	7.5
0.26	10.0
0.30	12.6
0.34	15.0
0.38	17.7
0.42	20.0
0.45	22.5
0.49	25.0

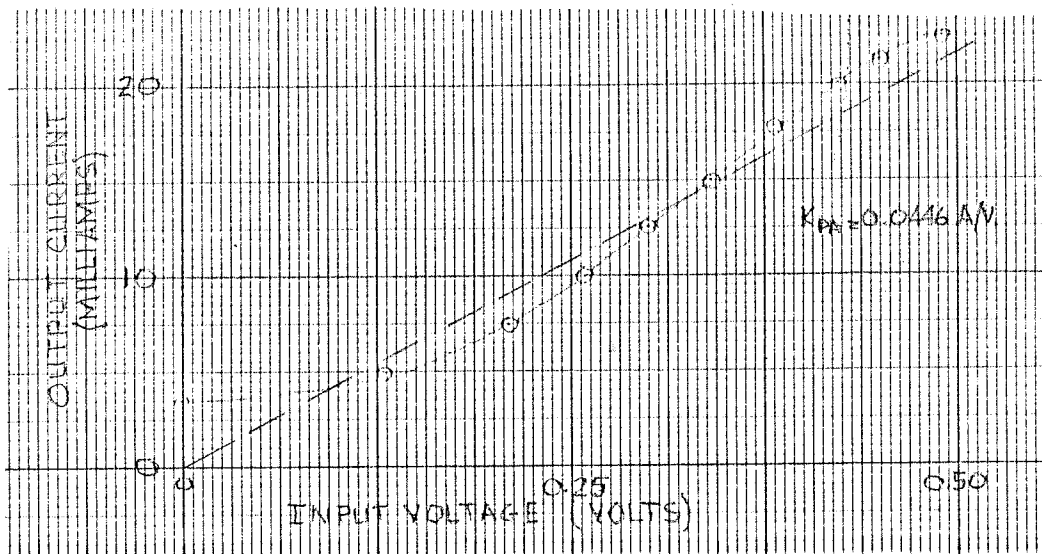


Figure 2-7: Static characteristic of the power amplifier.

The power amplifier characteristic may be combined with the dynamometer characteristic and approximated by

$$K_{p.a.} = 0.0446 \text{ amps./volt}$$

The dynamometer characteristic then becomes

$$T_o = K_o I_{in}^2$$

where $K_o = 247 \text{ n.m./amp}^2$ for inputs to the power amplifier greater than zero,

and $K_o = 0$ for inputs to the power amplifier less than zero.

5) High Gain D.C. Amplifier

Due to the low values of signals from the torque

sensor, a high gain D.C. amplifier is necessary to amplify these signals to a workable level. The amplifier chosen was a Cohu Amplifier. The nameplate data are given in Appendix A. The amplifier has a gain which can be varied in steps of ten, from one tenth to one hundred thousand.

B) Dynamic Characteristics of the Components.

The dynamic characteristics of the components were obtained by applying a step to the input and observing the output. In all cases, the output had the form shown in Figure 2-8.

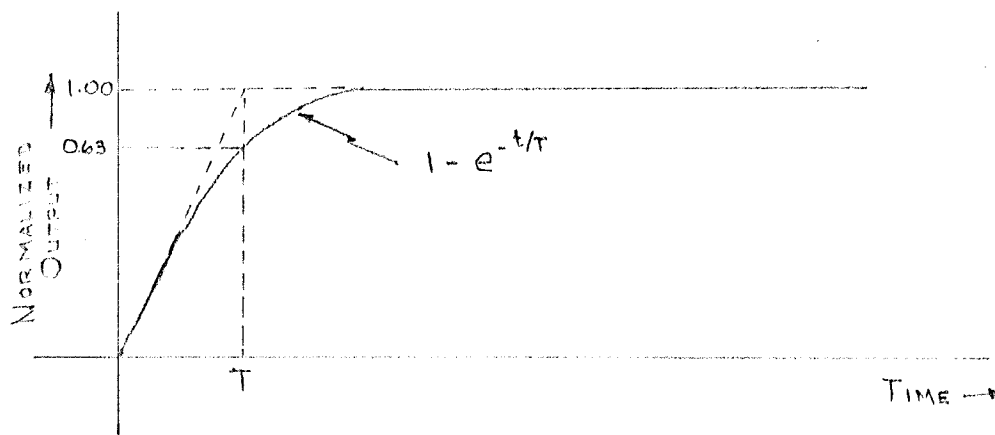


Figure 2-8: Response of a typical component to a step input.

The transfer function of each component is given in Table 2-5.

Table 2-5: Transfer functions of the components.

Component	T (m.sec.)	Transfer Function
Torque sensor	0.5	K_{ts}
Dynamometer	31.0	$\frac{K_o}{1 + 0.031 s}$
Power amplifier	0.2	K_{pa}
D. C. Amplifier	222.0	$\frac{K_a}{1 + 0.222 s}$

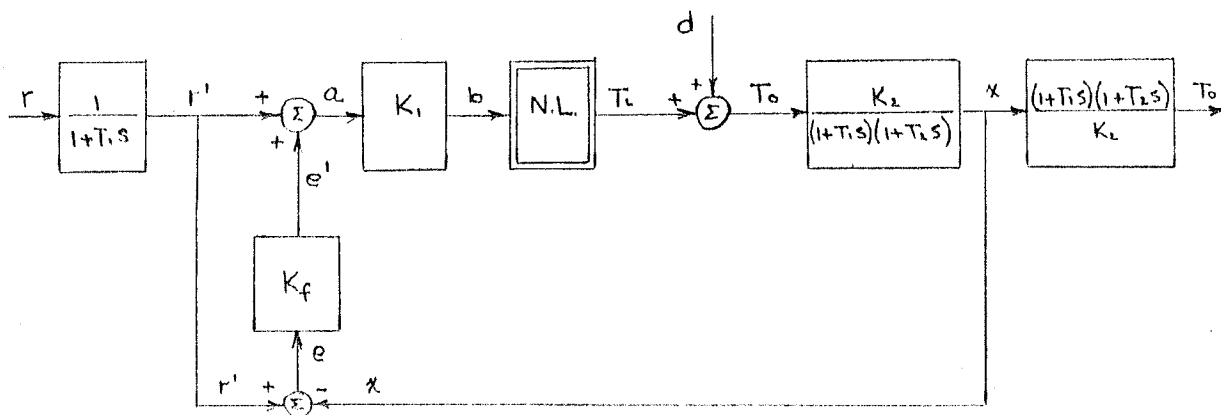
Note that since the time constants of the torque sensor and power amplifier are small compared to the dynamometer and D.C. amplifier, their transfer functions were approximated by a pure gain.

In Chapter III, the system will be analyzed to determine its response.

CHAPTER III
ANALYSIS OF THE SYSTEM

Because of the non-linearity of the dynamometer characteristic, phase plane analysis will be used to study the response of the system. The analysis will be confined to the case of the desired output equal to a constant. The response for this case will be indicative of the response for other inputs.

In order to facilitate the writing of the differential equations of the system, the block diagram of Figure 2-2 is shown in an equivalent form in Figure 3-1.



r =reference input (equal to desired output)

T_L =load torque

T_0 =output torque

d =disturbance (accelerating torque)

Figure 3-1: Equivalent block diagram of the proposed system.

The transfer function of the system from T_L to T_o is

$$\frac{T_o}{T_L} = 1 + \frac{J_L \dot{n}}{T_L} = K_3 (\dot{n}, T_L) \quad 3-1$$

This section of the system may be looked upon as a device having a gain which varies with \dot{n} and T_L in the manner given by equation 3-1.

The system will be analyzed with x as the output variable (see Figure 3-1 for x), and then T_o obtained from the equation

$$T_o = \frac{x + (T_1 + T_2) \dot{x} + T_1 T_2 \ddot{x}}{K_2} \quad 3-2$$

where T_1 and T_2 are the system time constants given in Table 2-5.

Analysis of the System

For simplicity, the analysis will be carried out with the motor torque equal to zero. Results for cases when the motor torque is not equal to zero may be deduced from this case.

The differential equation of the system may be written from inspection of Figure 3-1.

$$x + (T_1 + T_2) \dot{x} + T_1 T_2 \ddot{x} = K_2 T_o$$

$$T_o = K_3 T_L$$

$$T_L = K_o b^2$$



$$b = K_1 a$$

$$a = r'(1+K_f) - K_f x$$

where K_f is the feedback gain shown in

Figure 3-1.

Combining the above equations

$$x + (T_1+T_2) \dot{x} + T_1 T_2 \ddot{x} = K_0 K_1^2 K_2 K_3 \left[K_f^2 x^2 - 2K_f(1+K_f)r'x + (1+K_f)^2 r'^2 \right] \quad 3-3$$

where $K_3 = 1 - J_L/J_t$ for motor torque

equal to zero.

Rearranging equation 3-3

$$\ddot{x} + C_1 \dot{x} + f(x) = 0 \quad 3-4$$

$$\text{where } C_1 = \frac{T_1 + T_2}{T_1 T_2}$$

$$f(x) = \frac{-K K_f^2 x^2 + 1 + 2K K_f (1+K_f) r' x - K (1+K_f)^2 r'^2}{T_1 T_2}$$

$$\text{and } K = K_0 K_1^2 K_2 K_3$$

In the plane \dot{x} vs. x , the slope of a trajectory at any point is

$$\frac{d\dot{x}}{dx} = \frac{\ddot{x}}{\dot{x}} = \frac{-[C_1 \dot{x} + f(x)]}{\dot{x}} \quad 3-5$$

The trajectories may now be obtained graphically by the method shown in Appendix B. Figure 3-2 shows the calculated phase plane portrait for the constants given.

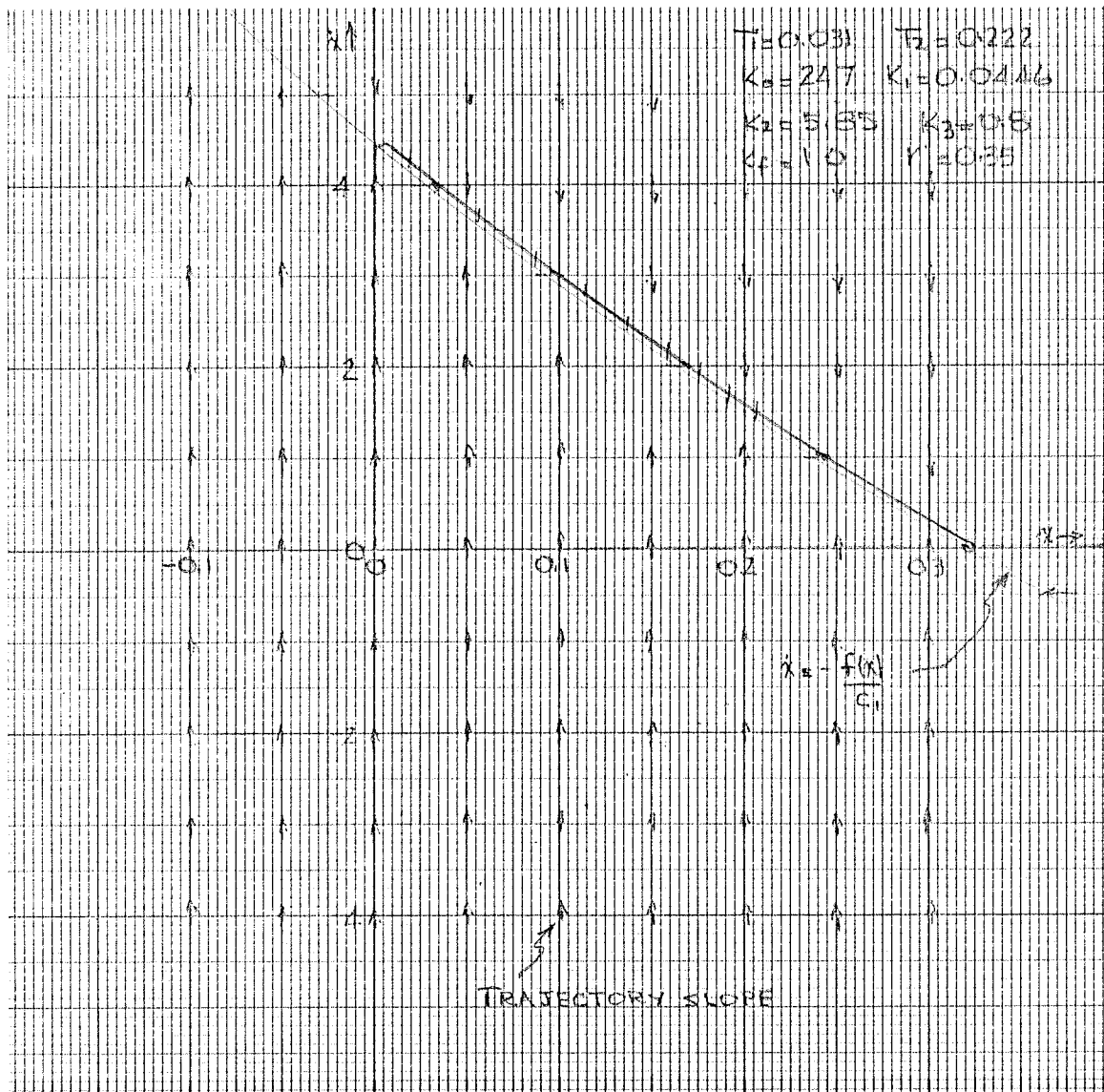


Figure 3-2: Phase plane portrait for the system of equation 3-4.

In obtaining this portrait, it was assumed that the time constant T_1 was small compared to the overall system time constant, so that r' was approximated by a step.

It is important to note that if the gain of the system is set to give the desired output at steady state (no accelerating torque), then the presence of acceleration results in a change in gain of K_3 , thus causing an error. This is apparent in Figure 3-2, where the final output is seen to be approximately 0.325, while it is desired to have the output equal to the input (0.35).

The output torque, T_o , may now be obtained from equation 3-2 and time scaling on the phase plane plot. Calculation of the output torque is shown in Table 3-1, and the output torque is shown plotted in Figure 3-3.

Table 3-1: Calculation of the output torque.

Time (m.sec.)	x/K_2	$(T_1+T_2)\dot{x}/K_2$	$T_1T_2\ddot{x}/K_2$	T_o (volts)
00.0	0.00	0.00	0.00	0.00
11.4	0.00	0.19	+0.44	0.63
22.8	0.01	0.16	-0.06	0.11
34.5	0.02	0.14	-0.06	0.10
45.9	0.02	0.12	-0.04	0.10
57.4	0.02	0.11	-0.05	0.08
68.8	0.03	0.10	-0.03	0.10
80.2	0.03	0.08	-0.03	0.08
91.6	0.03	0.07	-0.02	0.08
∞	0.055	0.00	-0.00	0.055

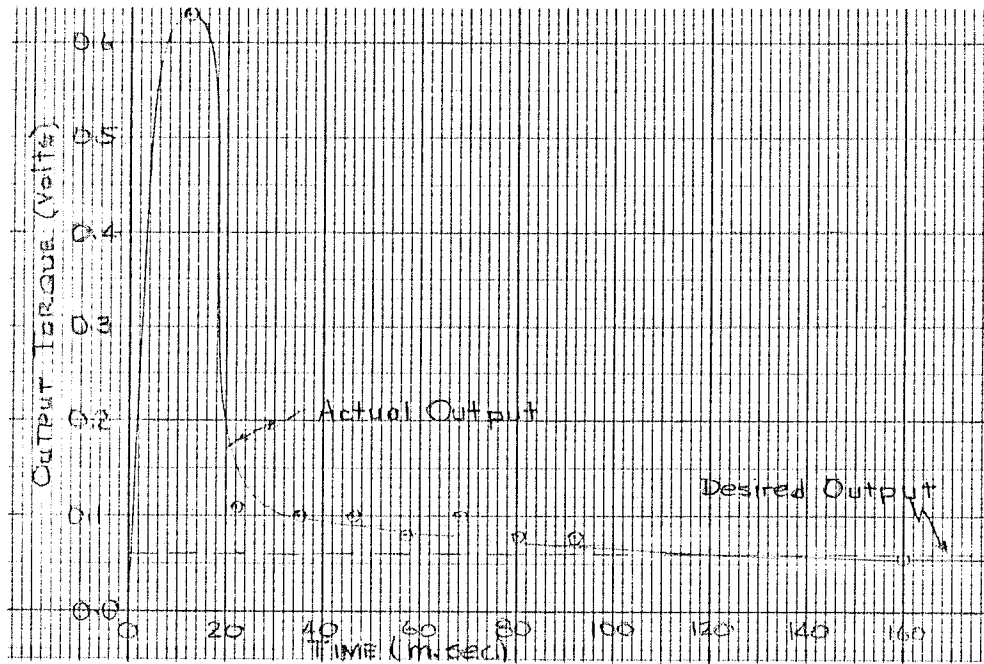


Figure 3-3: Response of the system to a step input
(motor torque equal to zero)

In Chapter IV, an attempt will be made to compensate for the undesirable characteristics of the system and to reduce the error.

CHAPTER IV

COMPENSATION OF THE SYSTEM

Examination of Figure 3-3 reveals two outstanding defects in the response of the system. These are the steady state error in the presence of acceleration, and the large overshoot in response to a step input.

In order to study the response of the system more closely, with a view towards compensating for these defects, the block diagram of Figure 2-1 was simulated on an analog computer. Using the computer setup shown in Figure 4-1, it was relatively simple to change time constants and gains to determine the compensation necessary to improve the response to a desirable level of accuracy. The effect of the presence of motor torque was also determined with no additional difficulty.

As stated in Chapter II, the performance index is to be the Integral Squared Error. As a level of accuracy, two percent of the desired integral squared output was chosen.

Effect of Changes in System Parameters

As a check on the accuracy of Figure 3-3, the response of the system to a step (motor torque equal to zero) is shown in Figure 4-2. Also included in this figure is the

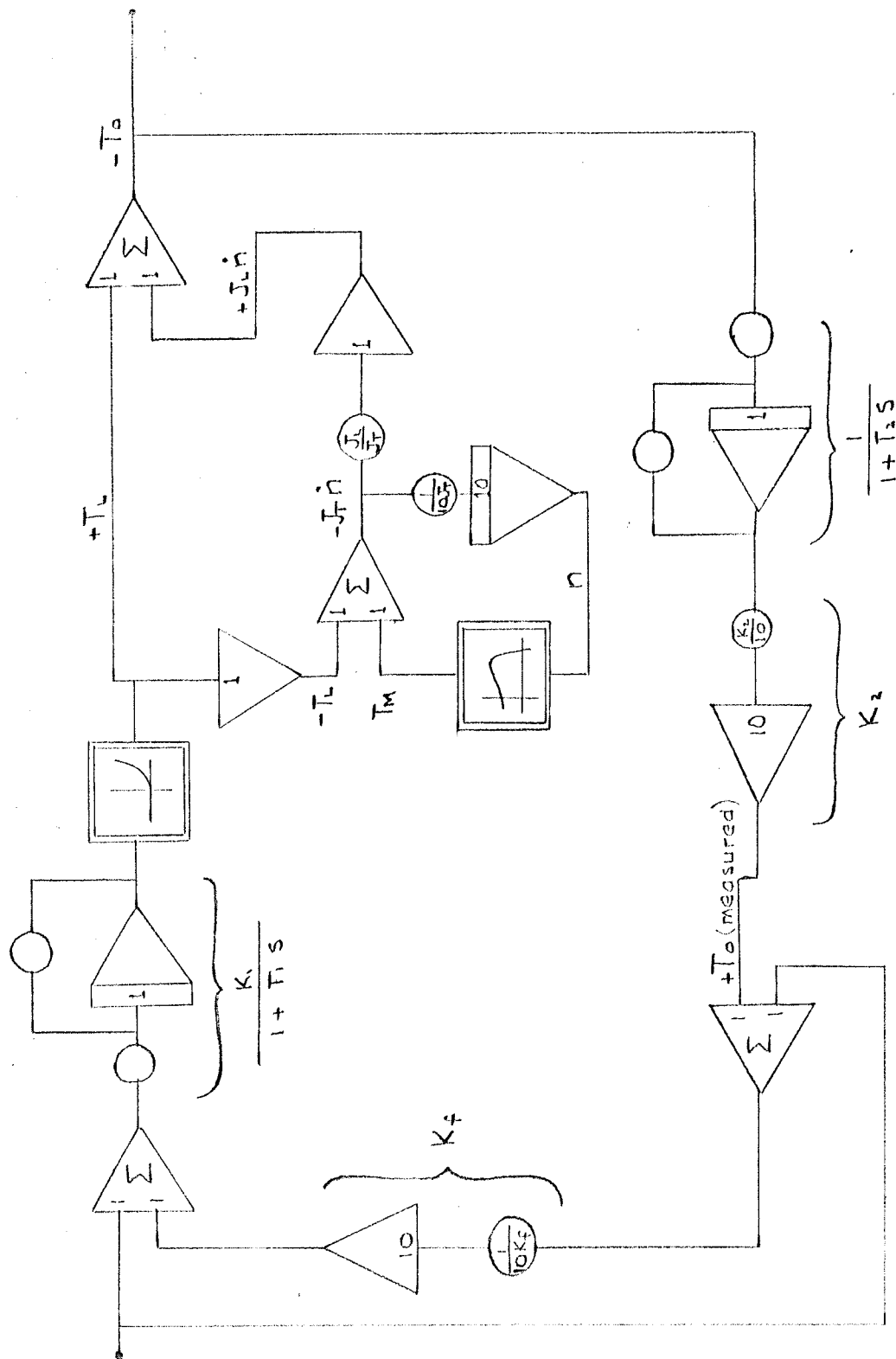


Figure 4-1: Schematic diagram of the analog computer simulation of the system.

effect of changing the feedback gain, K_f .

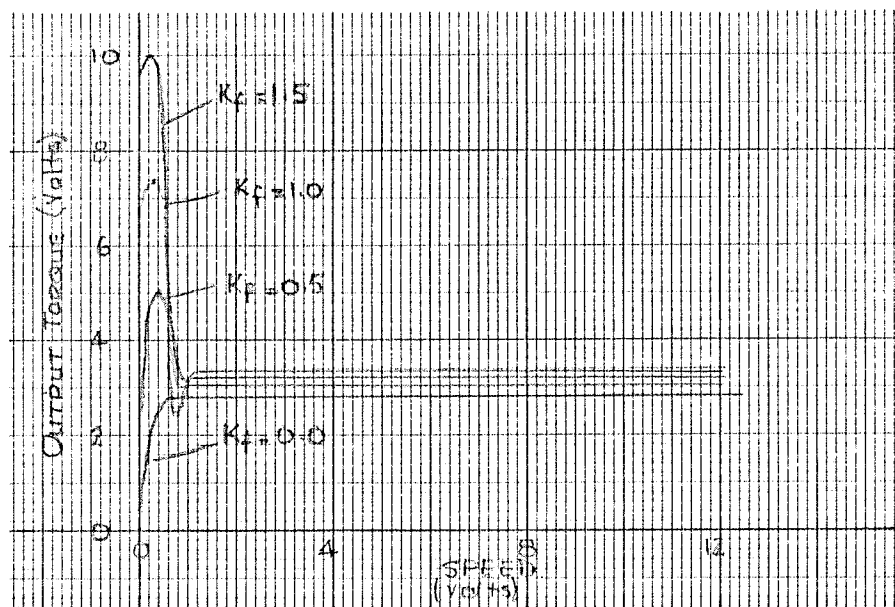


Figure 4-2: Response of the system to a step
(motor torque equal to zero)

Figure 4-2 shows that increasing the feedback gain reduces the steady state error, but increases the overshoot. As a method of compensation, therefore, this alone is unsatisfactory.

Figure 4-3 shows the output of the system including the effects of motor torque. Again, the reduced error and increased overshoot is apparent.

The effects of reducing the time constant T_2 was next observed. It was found that reducing the time constant reduced the overshoot, but had no effect on the steady state error. The combined effect of increasing the

feedback gain and reducing the time constant is shown in Figure 4-4. Figure 4-4 was obtained from oscilloscope traces.

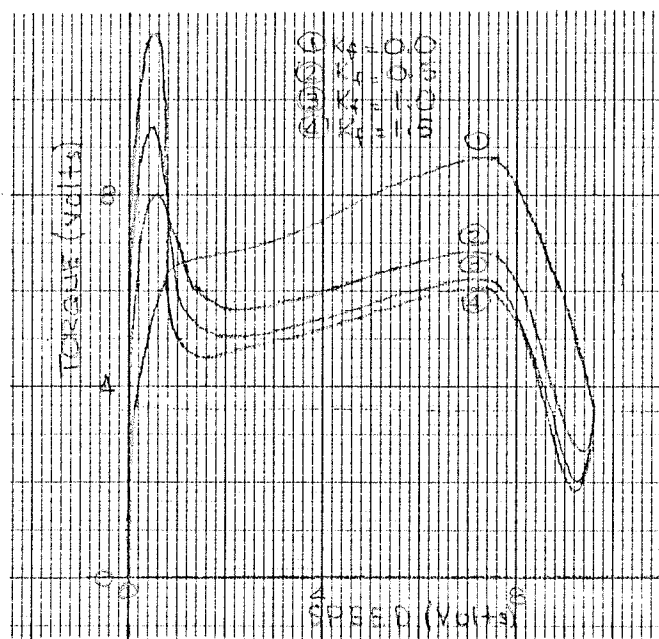


Figure 4-3: Response of the system to a step with effects of motor torque included.

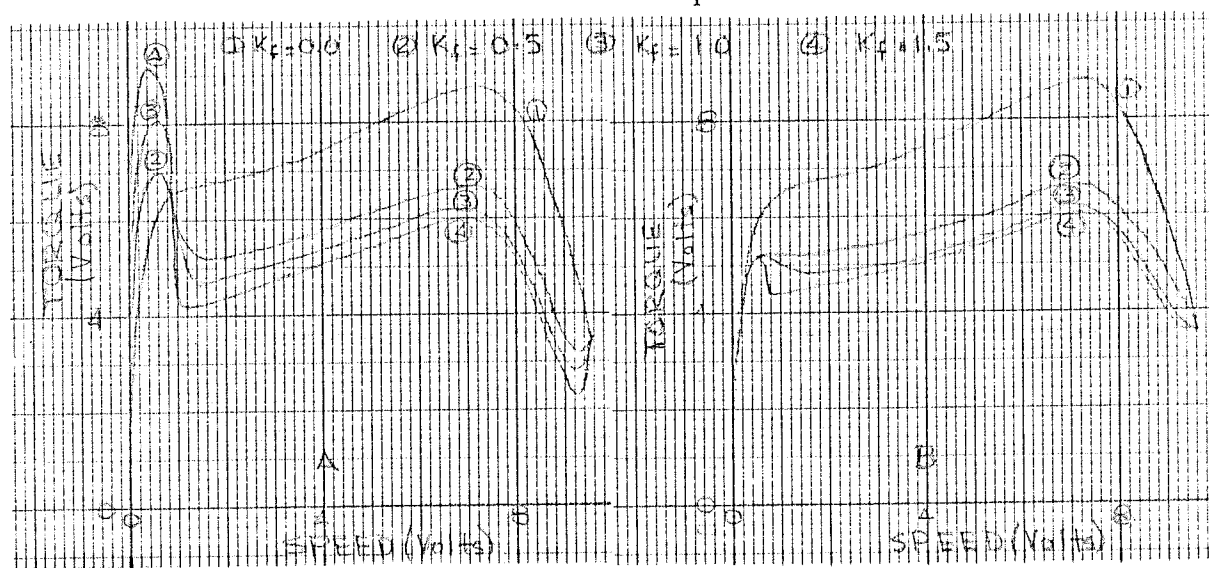


Figure 4-4: Response of the system after compensation.

A) $T_2 = 0.122$

B) $T_2 = 0.022$

The Integral Squared Error for the compensated system is shown plotted against feedback gain in Figure 4-5. The error was obtained graphically from Figures 4-3 and 4-4.

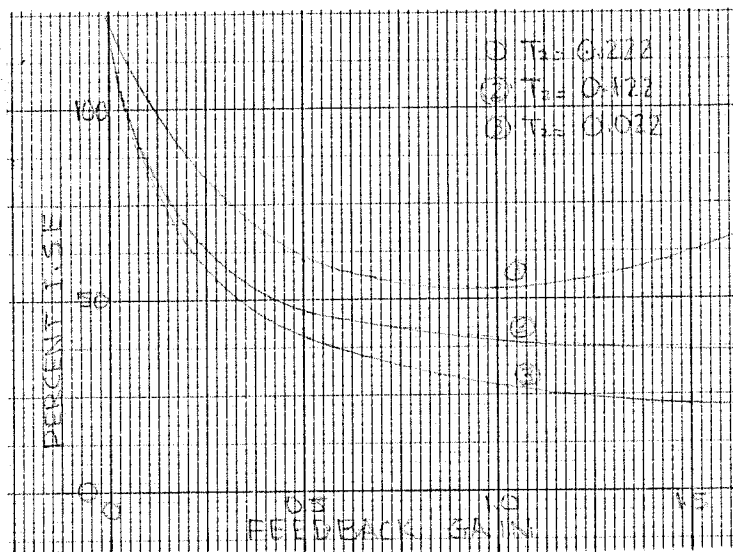


Figure 4-5: The Integral Squared Error as a function of feedback gain.

Figure 4-5 shows that there is very little reduction in the Integral Squared Error for feedback gains greater than unity.

Also, while reducing the error considerably, reduction of the time constant will not reduce the error to a satisfactory level.

The cause of most of the error appears to lie in the effective change in gain of the system due to the presence of acceleration.

Equation 3-1, relating the variation of gain with

\dot{n} and T_L , is shown plotted in Figure 4-6.

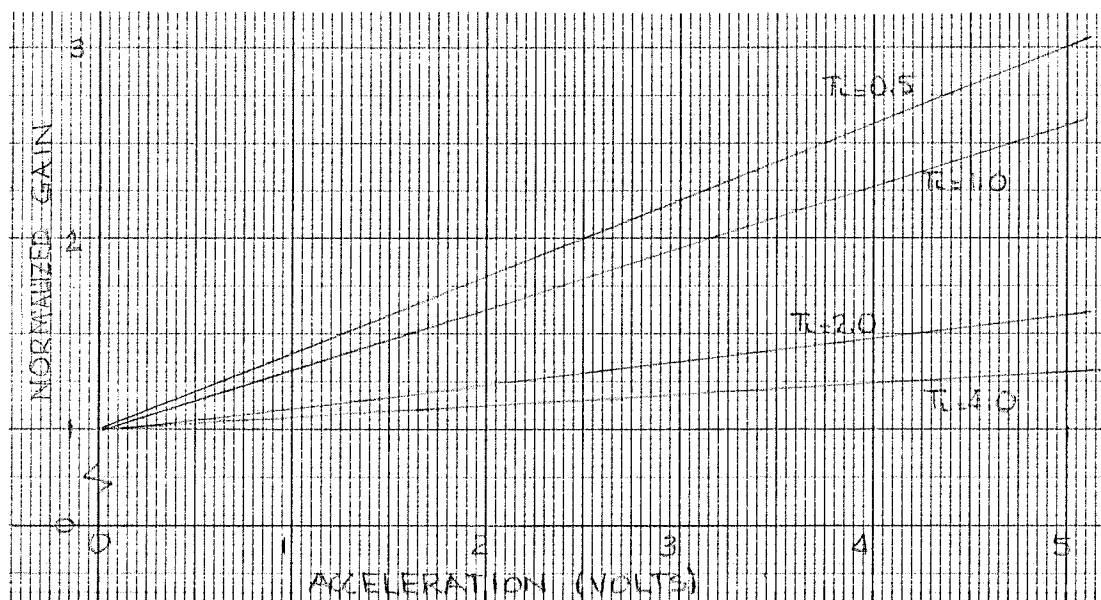


Figure 4-6: Normalized variation of the gain of the system due to the presence of acceleration.

Compensation for the above defect may be accomplished by inserting into the system, an amplifier which has a gain varying inversely as equation 3-1. Placing the amplifier before the dynamometer requires the relationship to be an inverse square root. The desired amplifier characteristic is shown in Figure 4-7.

The amplifier was simulated on the analog computer and the response of the system is shown in Figure 4-8. Since the whole family of curves could not be set up simultaneously, the proper characteristic was simulated for each load torque shown in Figure 4-8.

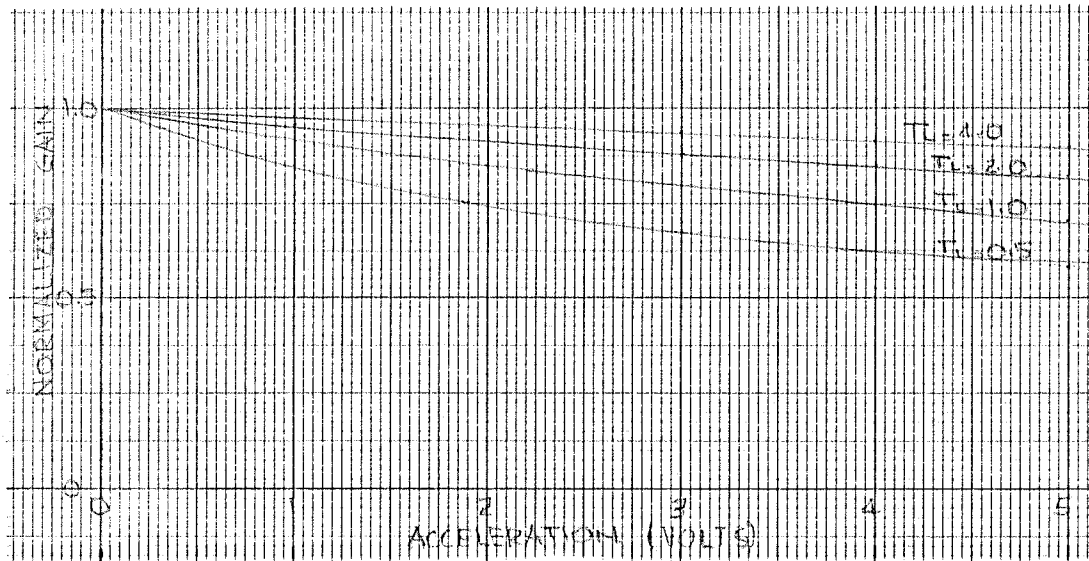


Figure 4-7: The desired compensating amplifier characteristic.

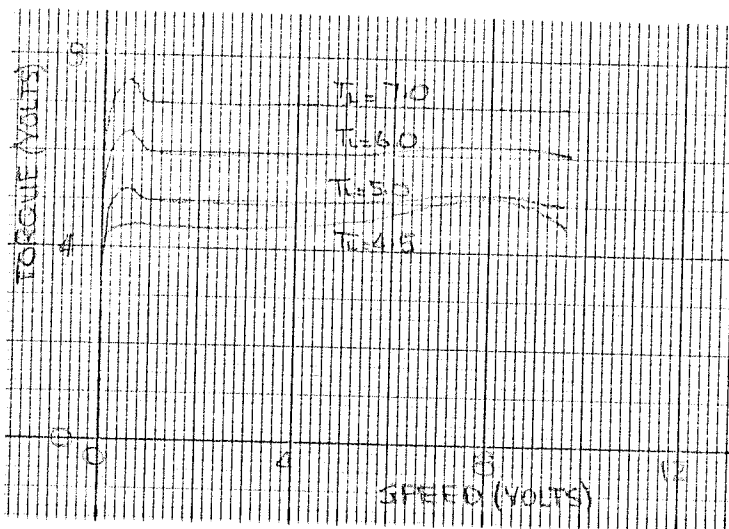


Figure 4-8: Response of the compensated system.

The Integral Squared Error for the load torques of Figure 4-8 are given below.

Table 4-1: The Integral Squared Error of the compensated system.

Load Torque (volts)	Integral Squared Error
7.0	0.17 percent
6.0	0.29 percent
5.0	0.42 percent
4.5	0.72 percent

Compensation of the Actual System

Tests on the actual system showed that reduction of the time constant T_2 to 0.122 sec. gave a similar response to Figure 4-4 A, with errors of the same magnitude as those given in Figure 4-5.

The compensation was achieved by placing a lead network in series with the Cohu Amplifier. The schematic diagram of the compensator is shown below.

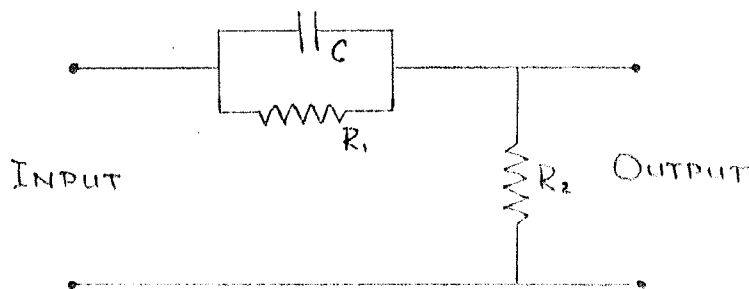


Figure 4-9: Schematic diagram of the compensator.

No attempt was made to design an amplifier with the characteristics of Figure 4-7, since the design would be beyond the scope of this thesis. However, since the other results agree so closely with those obtained from the analog computer, it is reasonable to assume that this form of compensation would reduce the errors to approximately those given in Table 4-1.

CHAPTER V

DISCUSSION AND CONCLUSIONS

The results of the attempts at compensation are summarized below.

- 1) Compensation by increasing the feedback gain alone reduces the steady state error, but increases the overshoot.
- 2) Decreasing the time constant, T_2 , reduces the overshoot, but does not affect the steady state error.
- 3) Compensation by a combination of the above methods improves the response of the system, but not to a satisfactory level.
- 4) The introduction of a variable gain amplifier improves the response of the system to a desirable level of accuracy.

A system such as the one designed might be found useful as an educational aid in an Electrical Machines Laboratory. Using a system similar to the one investigated here, motor characteristics could be obtained automatically. It would only be necessary to make the desired output a function of time rather than speed (for example a ramp), and the characteristic could be plotted automatically on an X-Y recorder. There are undoubtedly, several other

practical applications of a system such as this.

The response of the system was shown to be adequate for large load torques (small disturbances). However, as the disturbance increases, the response soon becomes unsatisfactory. Some attempt might be made at compensating the system even in the presence of large disturbances.

Because of the non-linear characteristic of the dynamometer, the gain of the system must be adjusted for each value of desired output. It might be possible to devise a scheme to eliminate the necessity of changing the gain with desired output, thus making the system fully automatic.



BIBLIOGRAPHY

- 1) Newton, G.C., Gould, L.A., Kaiser, J.F., Analytical Design of Linear Feedback Controls (John Wiley and Sons, Inc. New York 1957) pp. 39-41.
- 2) Gibson, J.E., Nonlinear Automatic Control (McGraw-Hill Book Co., New York 1963) pp. 237-246.
- 3) Gibson, J.E., Nonlinear Automatic Control (McGraw-Hill Book Co., New York 1963) pp. 251-253.

APPENDIX A

NAMEPLATE DATA OF THE COMPONENTS

Motor

Bodine Electric Co.

Three Phase Induction Motor

220 V., 0.3 A., 1/20 H.P., 60 c.p.s., 1725 r.p.m.

No. 249QE005 Type NPP-34

Continuous Duty 55C Temp. Rise

Dynamometer

Magtrol Inc. HC500

Rated current = 65 m.a. R(25C) = 1200 ohms

Torque at rated current = 100 in.oz.

Polar moment of inertia = 56.2×10^{-6} slug-ft.²

De-energized torque drag = 0.7 in.oz.

Torque Sensor

Lebow Associates Inc.

Model MTE-100 Serial No. 271

Capacity: 0 to 100 in.oz.

Speed: 0 to 20,000 r.p.m.

Tachometer

Servo Tek Products

Type SA-757A-2

7 volts/1000 r.p.m.

D.C. Amplifier

Cohu Electronics Inc.

Electronic Galvanometer

Model 204A Serial No. 5102

Sensitivity: $10\mu\text{V}$ or $.001\mu\text{A}$ F.S. on $\times 1$ range

Input Resistance: 10,000 ohms

Output: ± 1 volt full scale at 1 m.a. max.

APPENDIX B

A GRAPHICAL METHOD OF OBTAINING PHASE PLANE TRAJECTORIES

The phase plane trajectories corresponding to equation 3-5 may be obtained graphically by the following procedure.

$$\frac{d\dot{x}}{dx} = \frac{-[C_1 \dot{x} + f(x)]}{\dot{x}} \quad 3-5$$

- 1) Plot $\dot{x} = -f(x)/C_1$

Referring to Figure A-1, the vertical line from the curve to the point $P(x_1, \dot{x}_1)$ has the length

$$\dot{x}_1 + f(x_1)/C_1$$

- 2) The line is then turned 90 degrees and multiplied by C_1 by the construction shown. The angle ϕ is given by

$$\phi = \tan^{-1} \alpha C_1$$

$$\text{where } \alpha = \frac{\text{scale of } \dot{x}}{\text{scale of } x}$$

- 3) The line P-Q is then projected onto the x-axis. The line joining Q' to P then has the slope

$$\frac{\dot{x}_1}{C_1 \dot{x}_1 + f(x_1)}, \text{ and the desired slope is orthogonal to}$$

this.

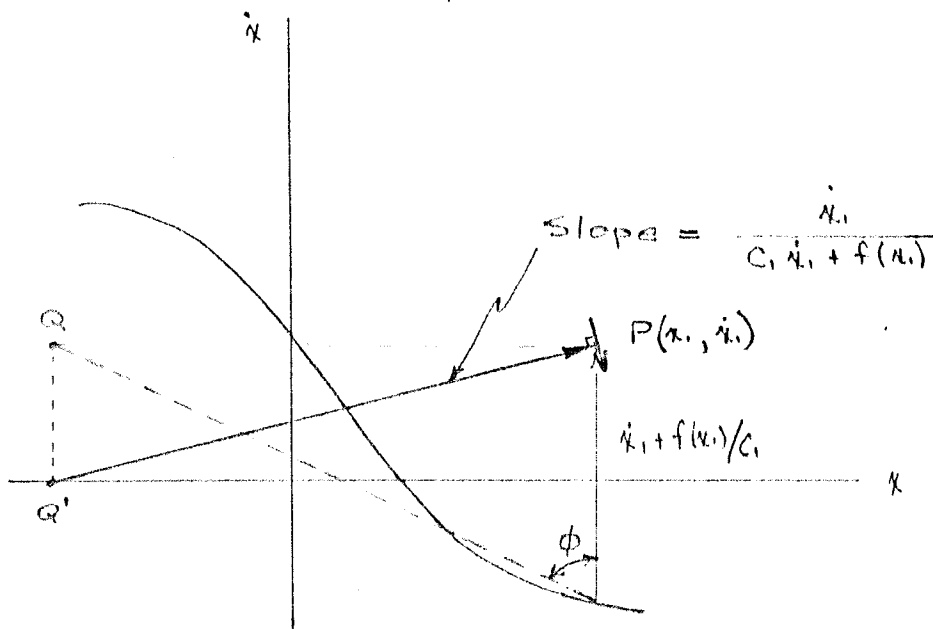


Figure B-1: An illustration of the graphical method for obtaining phase plane trajectories.

The calculations for the phase plane portrait of Figure 3-2 are shown below.

$$\text{For } r=0.35, K_0=247, K_1=0.0446, K_3=0.8,$$

$$K_2=5.85$$

$$K_0 K_1^2 K_2 K_3 = 2.30$$

$$T_1 + T_2 = 0.253$$

For $K_f = 1.0,$

$$-f(x)/C_1 = 9.08x^2 - 16.7x + 4.45$$

Table B-1: Calculation of $-f(x)/C_1$.

x	x^2	$9.08x^2$	$-16.7x$	$+4.45$	$-f(x)/C_1$
0.0	0.00	0.00	0.00	4.45	+4.45
0.1	0.01	0.09	-1.67	4.45	+2.87
0.2	0.04	0.36	-3.34	4.45	+1.47
0.3	0.09	0.82	-5.01	4.45	+0.26
0.4	0.16	1.45	-6.68	4.45	-0.78
0.5	0.25	2.27	-8.35	4.45	-1.63
0.6	0.36	3.27	-10.00	4.45	-2.28